Level Set Hyperspectral Image Classification Using Best Band Analysis

John E. Ball, *Student Member, IEEE*, and Lori Mann Bruce, *Senior Member, IEEE*

***Abstract*—We present a supervised hyperspectral classification procedure consisting of an initial distance-based segmentation method that uses best band analysis (BBA), followed by a level set enhancement that forces localized region homogeneity. The proposed method is tested on two hyperspectral images of an urban and rural nature. The proposed method is compared to the maximum likelihood (ML) method using BBA. Quantitative results are compared using segmentation and classification accuracies. Results show that both the initial classification using BBA features and the level set enhancement produced high-quality ground cover maps and outperformed the ML method, as well as previous studies by the authors. For example, with the compact airborne spectrographic imager image, the ML method resulted in accuracies $\leq 95.5\%$, whereas the level set segmentation approach resulted in accuracies as high as 99.7%.**

***Index Terms*—Band selection, classification, dimensionality reduction (DR), hyperspectral, image classification, image processing, level sets, remote sensing, segmentation, spectral angle mapper (SAM), spectral information divergence (SID), vicinal pixels.**

I. Introduction and Background

WHEN CREATING a thematic map (TM) from a hyperspectral image (HSI), neighboring pixels are often mislabeled, which can cause regions of homogeneous ground cover to appear heterogeneous. These errors can be caused by inadequate training data, natural class overlap, or high data dimensionality, i.e., the well-known Hughes phenomenon [1]. In order to mitigate effects of the Hughes phenomenon, a typical hyperspectral system will have a dimensionality reduction (DR) component, which seeks to simultaneously reduce the data dimensionality and to maximize the class separability. Commonly used DR methods include principal components analysis, linear discriminant analysis (LDA), independent component analysis, projection-based methods, and methods that reduce the hyperspectral data to a single scalar measure, including the spectral angle mapper (SAM) and spectral information divergence (SID) metrics [2]–[10].

In HSI classification, some popular approaches include metric-based methods, such as SAM and SID, contemporary methods such as maximum likelihood (ML), kernel-based methods such as support vector machines, and more recently, level set methods. The ML classification method [2], [6] is arguably the most commonly used method for remotely sensed image classification. In this paper, the authors investigate the SAM, SID, and ML, where best band analysis (BBA) will be used to mitigate the Hughes phenomenon. In addition, a level set approach will be used to enforce regional homogeneity in the TM. This paper is an extension of the authors' work in [3], [7], and [11].

Manuscript received October 8, 2006; revised June 18, 2007. The work of J. E. Ball was supported in part by the National Science Foundation, by Honda, and by the National Aeronautics and Space Administration.

J. E. Ball is with the Electromagnetic and Sensors Systems Department, Naval Surface Warfare Center, Dahlgren, VA 22448 USA (e-mail: john.e.ball@navy.mil).

L. M. Bruce is with the Department of Electrical and Computer Engineering and the GeoResources Institute, Mississippi State University, Starkville, MS 39762 USA (e-mail: bruce@gri.msstate.edu).

Color versions of one or more of the figures in this paper are available online at http://ieeexplore.ieee.org.

Digital Object Identifier 10.1109/TGRS.2007.905629

II. Level Sets

For 2-D image segmentation, the level set boundary is the zero level set of an implicit function ϕ defined as $\phi(x, y, t) : \Re^2 \times [0, T) \rightarrow \Re$, where $\Re$ is the set of real numbers, and T is some large maximum time value for the system. The time element is artificial and is used in the evaluation of partial differential equation (PDE) controlling the segmentation. The level set equation for front propagation with a 2-D speed function $\boldsymbol{F}(x, y)$, acting normal to the level set curve, is given by the PDE $\phi_t + \boldsymbol{F}|\nabla\phi| = 0$, where ϕ_t is the partial derivative of ϕ with respect to time, and $\nabla\phi$ is the gradient [12]. The level set evolves in accordance with the speed function $\boldsymbol{F}$, and it will continue to propagate outward (inward) as long as the speed function is positive (negative). A grid spacing $\Delta x = \Delta y = 1$ and time step $\Delta t = 0.8$ are used.

Dell'Acqua *et al.* extracted and tracked moving clouds using level sets [13]. Keaton and Brokish used level sets to segment roads in pan-sharpened IKONOS images [14]. In their approach, the speed function is controlled by a spectral similarity term comparing signatures to reference signatures. They obtained good results, but no automated methods were suggested for choosing the optimal parameters in their speed function. Their method worked well because of the large spectral and textural differences between roads and other groundcovers. A more general method would be required if other image endmembers are to be segmented.

In [3], [7], and [11], the authors utilized methodologies that are similar to those used in [14]. Reference [7] was a feasibility study that used simple methods, and the initial results were promising [around 80% overall accuracy (OA)]. The speed function was optimized using BBA and Fisher's LDA and stepwise LDA (SLDA) [11]. OAs increased to about 94%. In [3], the authors used the same methods as in [7] for the spectral similarity term, and they also used BBA and a modified form of SAM, which is called scaled SAM. The accuracies increased to just over 98%.

III. Methodology

In the proposed method, feature extraction and optimization, namely BBA with SLDA, is performed first in order to determine the best set of spectral bands that discriminate each TM class. Then, appropriate speed functions are created, and level set segmentation is performed. The following assumptions are made about using the level set segmentation based on best band SAM (BSAM) and best band SID (BSID) metrics. 1) Better results may be obtained by using BSAM and BSID versus SAM and SID, which use all of the bands. 2) The BBA method is restricted to a set of contiguous bands and is implemented as a fixed length sliding window. 3) A classifier using vicinal pixel information can perform better than a per-pixel-based classifier.

Assumption 1 is based on previous research [3], [8]–[10], which used various feature extraction methods, but all used some form of BBA. Assumption 2 is a compromise used to make the computation time reasonable. Although the absolute best results may be obtained from an exhaustive search, this is typically not feasible in HSI processing. In previous research, the authors found that band growing, where band groups were allowed to grow as long as the distance metric improved, provided slight accuracy improvements at the expense of considerably more computation time [3]. In this paper, the analysis is restricted to a fixed band group length and to consecutive bands. This approach was also used in [3] and [10].

Many times in HSI classification, there are regions of a ground cover class that are generally classified correctly, but the TM usually contains errors that are made up of small isolated groups of incorrectly classified pixels. By employing vicinal (i.e., spatial neighbor) pixel information, the resulting classification may be enhanced, and the accuracy improved. If the scene contains areas of mostly homogenous ground cover, then there should be homogenous classification of pixels in these areas. The challenge is to correct these types of classification errors without corrupting the actual natural borders between ground cover classes.

A. Initial Image Segmentation

Feature extraction and optimization is performed as follows. 1) For each class, analyze the training signature to determine which set of bands is the most effective for class separation. 2) Use SLDA to optimize the best set of features. 3) For each pixel, create a feature vector using the optimal reduced feature for each class. 4) Perform an initial pixel by pixel classification. 5) Enhance the initial classification using level sets to force region homogeneity. The BBA algorithm allows the user to select the discrimination metric (SAM or SID) and the class separation distance metric, which is either the area under the receiver operating characteristics curve (ROC A_Z) or Bhattacharyya distance (BD) [6].

The BBA algorithm uses a sliding window with a fixed band group length and analyzes the signatures using BSAM or BSID. The best bands are selected using ROC A_Z or BD. Then, the algorithm uses SLDA with forward selection and backward rejection [11]. This process is repeated for each class. For each class c and each pixel, let the optimal feature be $f^c_{x,y}$, which is scalar. Assuming that the image training data have C classes, then for each image pixel (x, y), a $[1 \times C]$ feature vector $\vec{f}_{x,y} = [f^1_{x,y}, \ldots, f^C_{x,y}]^{\mathrm{T}}$ is created. A minimum Euclidean-distance classifier is then used to perform initial segmentation.

TABLE I
Number of Samples of Training and Testing Data

MALL			FARM		
Class	Train	Test	Class	Train	Test
Buildings	49	49	Cement	77	83
Grass	500	2067	Cotton	544	12280
Paths	500	1761	Pasture	500	1198
Shadows	53	56	Pecans	500	849
Trees	500	2148	Pond	162	162
Water	494	1463	Road	376	459
			Shadows	65	101
			Shrubs	500	136
			Soybeans	758	17700
TOTAL	2096	7544	TOTAL	3482	32968

TABLE II
Experimental Band Lengths for Fixed Length Feature Optimization

Band Set [a]	Value	Used By [c]	Band Set [a]	Value	Used By [c]
$\boldsymbol{L}_0$	All [b]	**M / F**	$\boldsymbol{L}_6$	{40}	**M / F**
$\boldsymbol{L}_1$	{4}	**M / F**	$\boldsymbol{L}_7$	{60}	**M / F**
$\boldsymbol{L}_2$	{8}	**M / F**	$\boldsymbol{L}_8$	{70}	**F**
$\boldsymbol{L}_3$	{12}	**M / F**	$\boldsymbol{L}_9$	{80}	**M**
$\boldsymbol{L}_4$	{16}	**M / F**	$\boldsymbol{L}_{10}$	{100}	**M**
$\boldsymbol{L}_5$	{20}	**M / F**	$\boldsymbol{L}_{11}$	{20,16,12,8,4}	**M / F**

[a] Band sets are fixed lengths for the fixed length feature extraction procedure and starting lengths for the band growing feature extraction procedure. [b] Set $\boldsymbol{L}_0$ is all available bands, i.e. bands 1-191 for the Mall image, and 1-72 for the Farm image. [c] M=Mall image, F=Farm image

B. Level Set Segmentation Enhancement

After initial segmentation, level set segmentation enhancement is performed for each class, with the exception of roads and shadows. These two classes are not processed with the level set method, because roads are long and narrow, and shadows (at least, from trees and bushes) are very small, and both would be eroded by the proposed method.

For each class to be processed with the level set method, a 2-D stopping map is created by treating the BSAM or BSID feature for each pixel as a random variable and by examining the cumulative distribution function (cdf). Let $F_c(x)$ be the cdf for class c, and τ_c be the smallest value of x with $F_c(x) \geq \beta$, where $\beta = 0.9996$ was experimentally chosen. Selecting a value of β close to 1.0 will account for almost all of the training data. If a smaller value of β is chosen, then the level set will not process larger values in the cdf and will provide a more conservative approach. The stopping map for class c is given by $G^c_{x,y} = H(f^c_{x,y} - \tau_c)$, where $H(\cdot)$ is the Heaviside step function. The 2-D image $G^c_{x,y}$ will be 1 if the pixel's feature vector for that class is suitably small, and 0 otherwise. As a final preprocessing step, the image $G^c_{x,y}$ is convolved with an isotropic Gaussian filter with unity variance and $[11 \times 11]$ region of support, which is denoted as G_σ. This filtering is frequently used in level set applications to provide smoothing.

TABLE III
MALL IMAGE EXPERIMENTAL RESULTS—OAS IN PERCENT

PDM [a]	SDM [b]	Classifier [c]	Overall Accuracies in percent versus the Band Set (reference Table II). Band sets are indicated below. The best result for each row is shown in boldface, the overall best result is shown with heavy border, and cases where the level set results are statistically better than the initial segmentation (i.e. Z-statistic is greater than 1.96) are shaded.										
			L_0	L_1	L_2	L_3	L_4	L_5	L_6	L_7	L_9	L_{10}	L_{11}
BSAM	R	Initial	96.75	90.27	91.62	93.74	95.43	96.53	96.88	**97.57**	96.67	96.73	89.90
BSAM	R	Level Set	96.92	90.23	91.21	94.94	96.66	97.79	97.10	**97.96**	97.30	97.19	90.12
BSAM	B	Initial	96.74	90.47	91.65	93.98	94.83	94.95	96.71	**97.60**	97.57	95.77	89.65
BSAM	B	Level Set	97.08	90.73	91.34	93.64	94.76	94.34	96.99	**98.12**	98.06	96.02	89.13
BSID	R	Initial	95.51	89.90	91.89	93.19	93.44	94.45	93.81	96.34	97.35	**97.55**	95.97
BSID	R	Level Set	95.64	90.12	92.97	93.78	93.69	94.00	93.68	96.91	97.68	**98.02**	96.66
BSID	B	Initial	95.74	89.65	90.76	93.82	93.04	93.33	94.60	96.13	**97.39**	95.55	94.72
BSID	B	Level Set	95.89	89.13	91.62	94.62	93.29	93.62	94.47	96.73	**97.92**	96.12	94.66
ML	MJ	ML	94.71	90.31	95.51	92.17	90.32	89.30	91.04	93.53	95.04	95.23	90.31
Best results from [26]			86.06										
Best results from [27]			94.20										
Best results from [17]			98.20										

[a] PDM is the pixel discrimination metric (BSAM or BSID for level set analysis, or ML=maximum likelihood)
[b] SDM is the statistical-based class discrimination metric (R=ROC, B=BD, MJ=MCJMD)
[c] ML=maximum likelihood.

The final stopping map is $\tilde{G}^c_{x,y} = \tilde{G}^c_{x,y} \otimes G_\sigma$, where $\otimes$ is the convolution operator.

An $[11 \times 11]$ sliding template is used to scan the area around each pixel in the segmentation TM (the size was chosen experimentally). For each class c, the template counts the total number of pixels assigned to that class, which is divided by the total number of pixels. For pixels near the border, the total number of pixels is the sum of the template pixels that are in the original borders of the image. Thus, for each pixel (x, y) and a class c, the following equation is evaluated:

$$T^c_{x,y} = \sum_{\Omega(x,y)} \delta\{\text{TM}_{x,y} - c\} / \|\Omega(x,y)\|$$

where $\text{TM}_{x,y}$ is the TM entry at location (x, y), $\Omega(x, y)$ is the set of "on" pixels in the template, δ is the Dirac delta function, and $\|\Omega(x, y)\|$ is the number of "on" pixels in the template. This creates a 2-D image for each class. For each pixel, a threshold is applied:

$$\tilde{T}^c_{x,y} = T^c_{x,y} - \alpha_T \tag{1}$$

where $\alpha_T = 0.5$ was selected to force the masks to have a majority of "on" pixels. Thus, (1) forces pixels with surrounding areas with less than a majority of similar pixels to have a threshold < 0.

The level set will not enter a region where the speed function is 0, and it will leave areas where the speed function is negative. In the following level set algorithm, the constant in step 1 was determined experimentally, and k is a loop variable:

1. **For** $k = 1$ to 3
2. Compute the speed function: $F^c_{x,y} = \tilde{T}^c_{x,y}\tilde{G}^c_{x,y}$
3. Run level set until no sign changes
4. **End For**

In order to compare the proposed methods to a well-known segmentation technique, the ML classifier is also used. In this case, BBA is also performed, and for the given band constraints (starting band length and whether to grow bands or to keep constant length), the band set with the best MCJMD metric will be used. ML is commonly used in remote sensing [2] and will provide a meaningful comparison for the BSAM and BSID results.

C. Experimental Data and Experiments

Two images are studied in this analysis. The "Mall" image is an urban image of the mall area in Washington D.C., USA and was collected using the Hyperspectral Digital Imagery Collection Experiment sensor on August 23, 1995. The image was subset into a 129 row by 235 column by 191 band image (19 noisy bands were removed) containing endmembers that are easily separated (water) and others which are more difficult to classify correctly (i.e., grass and trees).

The "Farm" image was taken by the Compact Airborne Spectrographic Imager [15] and was cropped to 315 rows by 1010 columns with 72 hyperspectral bands from approximately 414 to 954 nm with 8-nm spectral resolution. The image was taken from a rural farm area in Brooksville, Mississippi, USA, on July 1, 2002 in good weather conditions. The image is a scene of the Black Belt Branch Experiment Station where field-level agricultural experimental studies are conducted. The crops have a high level of natural and imposed variations; therefore, the ground cover classes are very challenging to segment and classify.

Table I lists the number of training and testing signatures for each class for both images. Experiments are performed for various combinations of BSAM, BSID, ROC A_Z, and BD, and the various band group lengths are defined in Table II. Band set L_0 includes all bands, and L_1–L_5 were chosen to analyze small local features in the data set, while band sets L_6–L_9 look at a larger number of bands. The band sets were chosen in a previous work by the author based on the characteristics from the mall image [3]. For instance, the large main peaks of trees and grass are approximately 20 bands wide, the red edge is approximately 4 bands wide, and the small peaks in the main large peak are approximately 8–12 bands wide. L_{10}

TABLE IV
FARM IMAGE EXPERIMENTAL RESULTS—OAS IN PERCENT

PDM [a]	SDM [b]	Classifier [c]	Overall Accuracies in percent versus the Band Set (reference Table II). Band sets are indicated below. The best result for each row is shown in boldface, the overall best result is shown with heavy border, and cases where the level set results are statistically better than the initial segmentation (i.e. Z-statistic is greater than 1.96) are shaded.									
			L_0	L_1	L_2	L_3	L_4	L_5	L_6	L_7	L_8	L_{11}
BSAM	R	Initial	94.16	91.96	96.93	98.46	96.36	**97.60**	96.45	94.35	94.29	97.55
BSAM	R	Level Set	98.67	98.19	99.47	99.53	98.63	**99.55**	99.37	98.64	98.60	99.51
BSAM	B	Initial	93.99	91.31	97.83	98.39	**98.44**	98.28	96.37	94.07	94.07	98.33
BSAM	B	Level Set	98.61	97.76	99.45	99.56	**99.59**	99.57	99.31	98.38	98.59	99.58
BSID	R	Initial	90.80	92.37	96.64	97.98	97.38	**98.10**	96.11	90.93	91.13	96.61
BSID	R	Level Set	96.93	98.30	**99.58**	99.56	98.97	**99.58**	99.33	96.24	96.37	99.53
BSID	B	Initial	90.48	89.82	97.28	98.16	**98.24**	97.57	96.04	91.32	90.55	97.59
BSID	B	Level Set	96.86	97.54	99.64	**99.70**	99.56	99.54	99.26	96.26	96.55	99.51
ML	MJ	ML	91.22	90.67	93.46	**95.52**	**95.52**	95.47	94.30	93.34	91.63	**95.52**

[a-c] See notes in Table III.

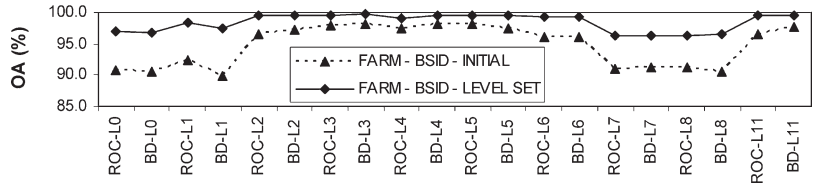

Fig. 1. OAs for the farm image using BSID metric. Note that similar results were obtained for BSAM metric.

is a combination of the smallest band sets. L_6–L_9 were added to test for Hughes phenomenon effects. To test the robustness of the proposed approach, the same band sets were also used to analyze the farm image (except for sets with more than 72 bands).

The results are analyzed in terms of OA for both the initial classification and the level set classification. A statistical analysis is also performed based on the confusion matrices (CMs), using a z-statistic method in [16]. A 95% confidence interval is used $(\alpha = 0.95)$, which gives a critical level of $z = 1.96$, and z-statistic values greater than 1.96 are considered statistically different.

Experimental parameter selection is discussed here. The isotropic filter region of support of size $[11 \times 11]$ is selected to allow the Gaussian filter to sufficiently decay at the edges. The process of picking a suitable window size is similar to the process required when using 2-D filtering methods. The appropriate window size depends on the size of the different regions in the image. The sizes of the band selection sliding template were initially chosen by hand after the examination of spectral signatures from the mall image. These values were then repeated for the farm image. Two suggested alternatives are given: to follow the aforementioned approach, and to examine spectral signatures from each class or to modify the procedure to utilize intelligent band grouping. To narrow the focus of this paper, the authors use fixed length windows. The cdf parameter β was chosen to allow some small overlap of the cdf of a given class with the other classes. The authors recommend to use a value of β near one.

IV. RESULTS AND DISCUSSION

The results for the mall image are shown in Table III. The worst results were just under 90% OA. The best results were

TABLE V
CONFUSION MATRIX FOR FARM IMAGE INITIAL SEGMENTATION. DIAGONAL ELEMENTS ARE BOLD

	Cem	Cot	Past	Pec	Pond	Road	Shad	Shrb	Soy
Cem	**0**	0	0	0	0	0	0	0	0
Cot	2	**8964**	0	0	0	0	0	0	21
Past	0	908	**830**	0	0	0	0	0	792
Pec	0	0	0	**601**	0	0	0	69	202
Pond	0	0	0	0	**162**	0	0	0	0
Road	81	33	0	0	0	**459**	0	0	0
Shad	0	2373	0	1	0	0	**101**	0	0
Shrb	0	0	0	43	0	0	0	**47**	1803
Soy	0	2	368	204	0	0	0	20	**14882**

Cem=Cement, Cot=Cotton, Past=Pasture, Pec=Pecans, Shad=Shadows, Shrb = Shrubs, Soy=Soybeans

TABLE VI
CONFUSION MATRIX FOR FARM IMAGE LEVEL SET SEGMENTATION. DIAGONAL ELEMENTS ARE BOLD

	Cem	Cot	Past	Pec	Pond	Road	Shad	Shrb	Soy
Cem	**80**	0	0	0	0	0	0	0	0
Cot	0	**12280**	0	15	0	0	1	0	42
Past	0	0	**1183**	0	0	0	0	0	0
Pec	0	0	2	**832**	0	0	0	20	0
Pond	0	0	0	0	**162**	0	0	0	0
Road	3	0	0	0	0	**459**	0	0	0
Shad	0	0	0	0	0	0	**100**	0	0
Shrb	0	0	13	0	0	0	0	**116**	0
Soy	0	0	0	2	0	0	0	0	**17658**

Cem=Cement, Cot=Cotton, Past=Pasture, Pec=Pecans, Shad=Shadows, Shrb = Shrubs, Soy=Soybeans

98.12% OA for BSAM, BD, and band set L_7. The results for ROC A_Z and BD are comparable. Only a few of the level set results are statistically different from the initial classification results (i.e., results with shaded background indicating a z-statistic greater than 1.96). This is because the ground cover classes in the mall image have relatively little natural variance, i.e., intraclass variance; therefore, regions of uniform ground

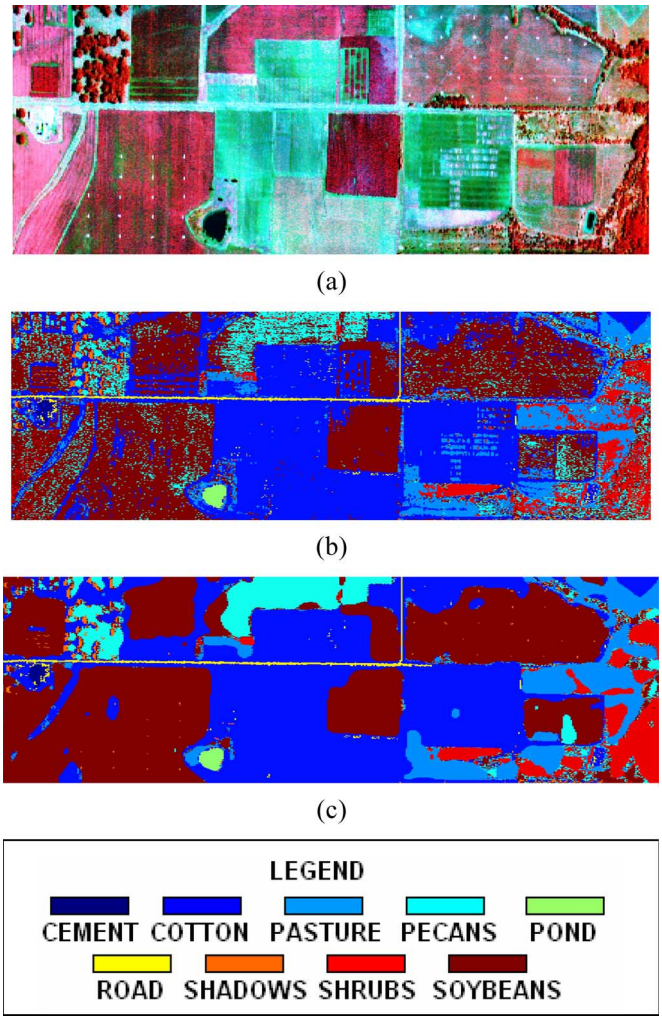

Fig. 2. Final TMs for the farm image. (a) Original image. (b) Initial segmentation. (c) Level set segmentation.

cover class are highly homogeneous after the initial segmentation and classification.

The farm image OA's are shown in Table IV, and the results show a drastic increase from the all-band (L_0) case for smaller band groups L_2–L_6. Larger band groups L_7 and L_8 performed worse than band groups L_2–L_6. This is most likely a manifestation of the Hughes phenomenon. The results for the midsized band groups were all above 95% OA. In general, the initial segmentation and level set results were better than the ML results. It is clear in Fig. 1 and Table IV that the level set method clearly provided an improvement in all cases, and it also provided a much more stable result (with respect to band group size) in terms of OA. All cases in Table IV are shaded, and in fact, the z-statistic was greater than 15 for all cases demonstrating a strong statistical significance. Tables V and VI show that the confusion matrix results are dramatically different with smaller off-diagonals. Fig. 2(a)–(c) shows the original farm image, best performing level set method result (BSID, BD, L_3) for the initial segmentation, and level set segmentation, respectively. Note how the speckle noise is removed from many of the fields, and how the regions have become more homogeneous.

For both images, the overall results are quite high and may not be as high in a large image if the training samples selected do not adequately describe the true class distributions.

V. Conclusion

The initial segmentations using BSAM and BSID were relatively accurate and outperformed the ML classifier. The results for ROC A_Z and BD are comparable, as well as for BSAM and BSID. When ground cover classes were relatively homogenous, as with the mall image, only a small improvement was provided by the level set method. However, when the ground cover classes were relatively heterogeneous, as with the farm image, the level set method provided a significant improvement, as evidenced by the high statistical differences based on the analysis of the corresponding CMs. Moreover, the application of the level set method made the OA's less sensitive to band group size and resulted in more homogenous ground cover classes, i.e., the results were less sensitive to natural intraclass variance in the vegetation classes.

Acknowledgment

The authors would like to thank the anonymous reviewers for their helpful suggestions.

References

[1] G. Hughes, "On the mean accuracy of statistical pattern recognizers," *IEEE Trans. Inf. Theory*, vol. IT-14, no. 1, pp. 55–63, Jan. 1968.
[2] D. A. Landgrebe, *Signal Theory Methods in Multispectral Remote Sensing*. Hoboken, NJ: Wiley, 2003.
[3] J. E. Ball and L. M. Bruce, "Level set hyperspectral segmentation: Near-optimal speed functions using band selection and scaled spectral angle mapper," in *Proc. IEEE Int. Geosci. Remote Sens. Symp.*, Jul. 2006, pp. 2596–2600.
[4] C. I. Chang, "An information-theoretic approach to spectral variability, similarity, and discrimination for hyperspectral image analysis," *IEEE Trans. Inf. Theory*, vol. 46, no. 5, pp. 1927–1932, Aug. 2000.
[5] C. Kwan, B. Ayhan, G. Chen, W. Jing, J. Baohong, and I. C. Chein, "A novel approach for spectral unmixing, classification, and concentration estimation of chemical and biological agents," *IEEE Trans. Geosci. Remote Sens.*, vol. 44, no. 2, pp. 409–419, Feb. 2006.
[6] R. O. Duda, P. E. Hart, and D. G. Stork, *Pattern Classification*, 2nd ed. New York: Wiley, 2001.
[7] J. E. Ball and L. M. Bruce, "Level set segmentation of remotely sensed hyperspectral images," in *Proc. IGARSS*, Seoul, South Korea, Jul. 2005, vol. 8, pp. 5638–5642.
[8] A. Cheriyadat, L. M. Bruce, and A. Mathur, "Decision level fusion with-bases for hyperspectral classification," in *Proc. IEEE Workshop Adv. Tech. Anal. Remotely Sensed Data*, 2003, pp. 399–406.
[9] A. Mathur, L. M. Bruce, and J. Byrd, "Discrimination of subtly different vegetative species via hyperspectral data," in *Proc. IEEE Int. Geosci. Remote Sens. Symp.*, Jun. 2002, vol. 2, pp. 805–807.
[10] S. Venkataraman, L. M. Bruce, A. Cheriyadat, and A. Mathur, "Hyperspectral dimensionality reduction via localized discriminant bases," in *Proc. IEEE Int. Geosci. Remote Sens. Symp.*, Seoul, Korea, Jul. 2005, vol. 2, pp. 1245–1248.
[11] J. E. Ball and L. M. Bruce, "Accuracy analysis of hyperspectral imagery classification using level sets," in *Proc. Amer. Soc. Photogramm. Remote Sens. Annu. Conf.*, Reno, NV, Apr. 2006. [Online]. Available: http://www.asprs.org/publications/proceedings/reno2006/
[12] J. A. Sethian, *Level Set Methods and Fast Marching Methods: Evolving Interfaces in Computational Geometry, Fluid Mechanics, Computer Vision, and Materials Science*, 2nd ed. Cambridge, U.K.: Cambridge Univ. Press, 2002.
[13] F. Dell'Acqua, P. Gamba, and P. Prevedini, "Level-set based extraction and tracking of meteorological objects in satellite images," in *Proc. IEEE Int. Geosci. Remote Sens. Symp.*, Jul. 2000, vol. 2, pp. 627–629.

[14] T. Keaton and J. Brokish, "A level set method for the extraction of roads from multispectral imagery," in *Proc. 31st Appl. Imagery Pattern Recog. Workshop*, Oct. 2002, pp. 141–147.
[15] ITRES Inc., *Compact Airborne Spectrographic Imager*, 2007. [Online]. Available: http://itres.com/cgi_bin/products.cgi
[16] R. G. Congalton and K. Green, *Assessing the Accuracy of Remotely Sensed Data: Principles and Practices*. New York: Lewis Publishers, 1999.

John E. Ball (S'03) received the B.S. degree in electrical engineering from the Mississippi State University, Starkville, in 1991, the M.S. degree in electrical engineering from the Georgia Institute of Technology, Atlanta, in 1993, and the Ph.D. degree in electrical engineering from the Mississippi State University.

Currently, he is a Civilian Engineer with the Naval Surface Warfare Center, Dahlgren, VA. His research interests include signal processing, level set-based segmentation algorithms, and image processing, particularly for mammographic and remotely sensed images.

Dr. Ball is a member of the IEEE Signal Processing and Geoscience and Remote Sensing Societies and has reviewed papers for the IEEE GEOSCIENCE AND REMOTE SENSING LETTERS and the IEEE TRANSACTIONS ON GEOSCIENCE AND REMOTE SENSING journals. He was a National Science Foundation Fellow from 2004 to 2006 and is a member of the Gamma Beta Phi, Tau Beta Pi, Phi Kappa Phi, and Eta Kappa Nu.

Lori Mann Bruce (S'91–M'96–SM'01) received the B.S.E. degree in electrical engineering from the University of Alabama, Huntsville, in 1991, the M.S. degree in electrical engineering from the Georgia Institute of Technology, Atlanta, in 1992, and the Ph.D. degree in electrical engineering from the University of Alabama, in 1996.

Currently, she is a Professor with the Department of Electrical and Computer Engineering, Mississippi State University, Starkville, where she also serves as an Associate Director for Research in the Geo-Resources Institute. Her research interests include applying advanced digital signal processing techniques such as discrete wavelet transforms to automated pattern recognition in hyperspectral remote sensing and digital mammography.

Dr. Bruce is a member of Eta Kappa Nu, Phi Kappa Phi, and Tau Beta Pi.